Numerical study of the movement of the knuckleball with rifle spin

Kanako Denbo and Tetuya Kawamura

(Received October 7, 2005)
(Revised December 30, 2005)

Abstract

In this study, the flow around the knuckleball with rifle spin is numerically simulated by solving the incompressible Navier-Stokes equations and computed the aerodynamics coefficients (i.e. drag, lift and side force coefficients) of the ball by using the results of flow calculations. These coefficients are computed for the different positions of the seam on the ball. The effect of this position and the rotation speed of the ball on the orbit are investigated. From the computations, we obtain numerically the "irregular change of the orbit" which is the most remarkable feature of the knuckleball. Also we find this feature appears even if the ball rotates several times per second suggesting the potential of the knuckleball with rifle spin which may be easier to throw than the ordinal knuckleball.

1. Introduction

The knuckleball used in the baseball game does not rotate very rapidly until it reaches a catcher. Although its speed is usually less than 100 km/h, the main feature of this ball is that its orbit is not simple. Therefore it is difficult to predict the orbit and a batter often fails to hit the ball.

We can find several experimental and numerical studies concerned with the behavior of the knuckleball [1]-[4]. In these studies, the axis of rotation is assumed to be perpendicular to the throwing direction of the ball as shown in fig.1 (a). This is due to the following reason, i.e. Mizoguchi et al [1] [2] analyzed the orbit of the knuckleball thrown by Wakefield who is a major-league pitcher by using video pictures and found that the ball rotates as mentioned above. Based on these studies, Himeno et.al numerically investigates the behavior of the knuckleball with such spin [3] [4].

On the other hand, Nishikiori et al. analyzed the orbit of the Wakefield's knuckleball one again and found another kind of knuckleball. The axis of rotation of this knuckleball is parallel to the thrown direction as shown in fig.1 (b). This knuckleball is called a knuckleball with rifle spin. Nishikiori also performed experimental studies of this knuckleball [5].

In this study, we tried to compute the flow around the knuckleball with rifle spin and investigate the effect of such rotation on the orbit of the ball since we cannot find numerical study of this kind of knuckleball.

2. Numerical Method

The goal of the present study is to determine numerically the orbit of the knuckleball with rifle spin. The ball continues to move under the effect of gravity and surrounding air. Therefore, it is necessarily to determine the force caused by the air as precisely as possible. This force is greatly affected by the position of the seam on the ball. In this study, we first calculate the force by changing its position variously. Then we compute the orbit by using these data of the force. We calculate under the assumption that the movement of a ball is quasi-steady, because the rotation of a ball is enough slow.

2.1 Calculation of the flow

The speed of the ball is small enough to assume the flow to be incompressible. Therefore, the governing equation is incompressible Navier-Stokes equation that is expressed in non-dimensional form as follows:

$$\nabla \cdot \mathbf{v} = 0 \tag{1}$$

$$\frac{\partial \mathbf{v}}{\partial t} + (\mathbf{v} \cdot \nabla)\mathbf{v} = -\nabla p + \frac{1}{\mathrm{Re}}\Delta \mathbf{v} \tag{2}$$

where **v** is the velocity, p is the pressure and $\mathrm{Re} = U / L/\nu$ is the Reynolds number based on the initial velocity of a ball U, the diameter of the ball and the kinematic viscosity of the air. The x direction is the direction of movement of a ball, while the z direction is the a positive vertical direction. The y direction is normal to both x and z directions. These equations are solved by the standard MAC method [6].

We used body fitted coordinate system in order to express the roughness of the ball. Figure 2 shows the grid system used in this study. This grid system is the same as that used by Himeno in the previous study [3] [4]. The number of the grid points is about one and half million (169 X 92 X 101). The far boundary is on the sphere of radius 20R where R is the radius of the ball.

Basic equations are transformed into generalized coordinate system (3) that enables us to use the grid indicated in fig.2.

$$\begin{cases} x = x(\xi,\eta,\zeta) \\ y = y(\xi,\eta,\zeta) \\ z = z(\xi,\eta,\zeta) \end{cases} \tag{3}$$

The transformed equation is solved in rectangular region by using finite difference method.

The nonlinear term is approximated by the third order upwind difference (4).

$$u\frac{\partial u}{\partial \xi}\bigg|_{\xi=\xi_i} = \begin{cases} u_i \cdot \dfrac{1}{6\Delta\xi} \cdot (2u_{i+1} + 3u_i - 6u_{i-1} + u_{i-2}) & u > 0 \\ u_i \cdot \dfrac{1}{6\Delta\xi} \cdot (-u_{i+2} + 6u_{i+1} - 3u_i - 2u_{i-1}) & u < 0 \end{cases} \tag{4}$$

This difference approximation can treat high Reynolds number flow stably without any turbulence model.

2.2 Calculation of aerodynamics coefficients

The aerodynamics coefficients are greatly affected by the position of the seam on the ball. We define the coordinate system as is shown in fig. 3 (a) where the x-axis is parallel to the moving direction of the ball and assume point A in fig. 3 (a) to be the base point of the ball. The position of the seam can be specified by the angle α and β shown in fig. 3 (b). If the unit normal at the point A is parallel to the x-axis, then α =0 and β =0. The force acting on the ball is specified by the three coefficients c_D, c_L and c_S. These are the normalized drag, lift and side force respectively. The directions of lift and drag force are opposite to gravity and the moving direction. The coefficient c_S is normal to both c_D and c_L. The calculations are performed in the framework that is fixed to the ball. Therefore, the ball is assumed to put into the flow of uniform speed U in this framework.

The grid system used in this computation is quite complicated as is shown in fig.3. Therefore, the effect of the angle α or β is taken into account in the computation by changing the direction of the uniform flow since the same grid system can be used. Then, the boundary conditions on the far boundary becomes as follows:

$$\begin{aligned} u &= -\mathrm{v}_0 \cos\beta' \cos\alpha' \\ v &= -\mathrm{v}_0 \cos\beta' \sin\alpha' \\ w &= -\mathrm{v}_0 \sin\beta' \end{aligned} \tag{5}$$

where $\alpha'(=\alpha)$ and $\beta'(=\beta)$ are defined in fig.4 (b). The direction of $\tilde{c}_S$ which is the side-force coefficient in this grid system is set to the direction of the uniform flow when $\alpha'=0^\circ$ and $\beta'=0^\circ$ as is shown in fig.4 (a). The direction of $\tilde{c}_L$ is opposite to the gravity and that of $\tilde{c}_D$ is normal both to $\tilde{c}_S$ and $\tilde{c}_L$.

The relation between (c_D, c_L, c_S) and $(\tilde{c}_D, \tilde{c}_L, \tilde{c}_S)$ is given by

$$\begin{bmatrix} c_D \\ c_L \\ c_S \end{bmatrix} = \begin{bmatrix} \cos\beta & -\sin\beta & 0 \\ \sin\beta & \cos\beta & 0 \\ 0 & 0 & 1 \end{bmatrix} \begin{bmatrix} \sin\alpha & 0 & \cos\alpha \\ 0 & 1 & 0 \\ \cos\alpha & 0 & -\sin\alpha \end{bmatrix} \begin{bmatrix} \tilde{c}_D \\ \tilde{c}_L \\ \tilde{c}_S \end{bmatrix}$$

$$
= \begin{bmatrix} \tilde{c}_D \sin\alpha\cos\beta - \tilde{c}_L \sin\beta + \tilde{c}_S \cos\alpha\cos\beta \\ \tilde{c}_D \sin\alpha\sin\beta + \tilde{c}_L \cos\beta + \tilde{c}_S \cos\alpha\sin\beta \\ \tilde{c}_D \cos\alpha - \tilde{c}_S \sin\alpha \end{bmatrix} \tag{6}
$$

2.3 Calculation of the orbit of the ball

If the velocity of the ball is $\mathbf{v}$, the equation of the motion of the ball becomes

$$
\frac{d\mathbf{v}}{dt} = \frac{1}{2m}\rho \mathbf{v}^2 A\mathbf{c} - \mathbf{g} \tag{7}
$$

where A and m are the cross section and mass of the ball, $\mathbf{c} = (c_D, c_L, c_S)$ is aerodynamics coefficient of the ball, ρ is the density of the air and the $\mathbf{g}$ =(0,g,0) is the gravity.

We assume that "the knuckleball rotates N times during its flight". We also assume that the angular velocity is constant for simplicity. The rotation angle becomes $2\pi N_{rps} t$ where N_{rps} is the number of rotation per unit time. The aerodynamics coefficients then become the function of time and are

$$
\mathbf{c}(t) = \begin{bmatrix} c_D(t) \\ c_L(t) \\ c_S(t) \end{bmatrix} = \begin{bmatrix} 1 & 0 & 0 \\ 0 & \cos(2\pi N_{rps}t) & -\sin(2\pi N_{rps}t) \\ 0 & \sin(2\pi N_{rps}t) & \cos(2\pi N_{rps}t) \end{bmatrix} \begin{bmatrix} c_D \\ c_L \\ c_S \end{bmatrix} \tag{8}
$$

We use this relation when we use $\mathbf{c}$ in equation (7). In this study, equation (7) is integrated by using the second order Runge-Kutta method.

The numerical procedure employed in this study can be summarized as follows:

(1) At first, aerodynamics coefficients are computed by solving the incompressible Navier-Stokes equation numerically for various angles of α and β. Large CPU time is required to obtain the time-averaged values. The values of α are 0,15,30,45,60,75 and 90 degree for β =0 and those of β are -90,-60,-30,0,30,60 and 90 degree for α =0. These values are chosen from consideration of symmetrical shape of the ball.
(2) The orbits of the ball are calculated for various cases from equation (7) by using aerodynamics coefficients obtained by the flow computations.

3. Results and discussions

3.1 Aerodynamics coefficients

The Reynolds number is fixed to 97000 that corresponds to the speed of the ball of 75km/h. Figures 5,6,7 show the dependence of α on the aerodynamics coefficients for β =0. These are drag, lift and side-force coefficients. The lines in the figure are our previous results while the points indicated by symbol "X" are our present results. The experimental results obtained by the wind-tunnel tests [1] [2] and computational results given by another author [3],[4] are also shown in the same figures for comparison. From these figures, we can find the agreement among numerical results is well. On the other hand, we can state following comments from the comparison of the experiments.
(1) For drag coefficients, the agreement in tendency is good although the computational values are generally small.
(2) For side-force coefficients, quantitative agreement is well but the absolute values are one half of experimental values or less.
(3) For lift coefficients, the absolute values are nearly the same but the sign becomes opposite when $\alpha > 45°$.

Considering the configuration of the ball, the computational results may be reasonable.

Figure 8 show the similar comparison for various angles of β in the case of α=0. Following results are obtained:
(4) For both drag and side-force coefficients, the agreement between computational results and experimental ones are rather good.
(5) On the other hand, discrepancy is found for lift coefficients.

One reason of this discrepancy is the effect of the rod used in the experiments to support the ball in the wind tunnel. Since side-force coefficients are the most important to simulate the wavy motion which is the typical for the knuckleball, we use present results for the calculation of the orbit of the ball.

3.2 Calculation of orbit of the ball

Conditions of the computation of the orbit are as follows: the speed of the ball is 75km/s; initial angle between the moving direction of the ball and horizontal plane is 10 degree; the distance from the position of the pitcher and that of the catcher is 18.44m; the number of rotation during the flight of the ball is chosen to 0.5, 1 and 2, and the change of the orbits is investigated.

Figure 9 shows the orbits in the case of α and β=0. Figure 9(a) is the top view showing the effect of side force while fig.9 (b) is the side view showing the change of the distance from the ground during the movement. Figures 10 and 11 are the results of α=30, β=0 and α=0, β=-30 corresponding to fig.9.

In fig.9, the number of rotation N is not sensitive to the orbit in the perpendicular plane (i.e. in the c_L direction) while the large displacement is observed in the horizontal plane (i.e. in the c_S direction) especially in the case of small rotation although the change is monotonous. In figs. 10 and 11, N gives large effect on the orbit both in the perpendicular and horizontal plane. We can observe the wavy orbit in the horizontal plane.

3.3 Maximum displacement in the position

Figures 12(a) and (b) are the maximum displacement in the position in c_L and c_S direction obtained by the computation of the orbits respectively. From these figures, we can find the displacement is at least 1.5m in c_L direction and it is 0.4m in c_S direction in some cases.

4. Concluding remarks

In this study, we simulate the flow around the knuckleball with rifle spin and obtain the aerodynamics coefficients. These coefficients are computed by changing the positions of the seam on the ball. The orbits of the ball during its flight of 18.44m between a pitcher and a catcher are calculated and investigate the effect of the rotation on the orbit. The number of rotation is chosen to 0.5, 1 and 2 during its flight. The following results are obtained:
(1) For drag and lift coefficients, we can obtain reasonable results which agree well with previous computations and experimental results.
(2) For lift coefficient, discrepancy to the experiment is observed although the agreement to the previous computation is well.
(3) If the number of rotation of the ball is 0.5 and 1 during its flight of 18.44m, the ball curves left or right direction. If it is 2, horizontally wavy motion of the ball is observed.
(4) The change of the position of the seam greatly affects the orbit of the ball.
(5) We can find remarkable effect on the orbit even if the knuckleball with rifle spin has several rotations per one second.

From (3), we can obtain numerically the "irregular change of the orbit" which is the most remarkable feature of the knuckleball. The result of (4) indicates that the quite different orbit of the ball can be achieved by the same speed and the same style of pitching if the initial position of the seam is different. Considering the fact that it is very difficult to control the rotation of the knuckleball, the result of (5) suggests the potential of the knuckleball with rifle spin that is easy to throw since some rotations does not suppress the irregular motion of the knuckleball. Fig13 is the comparison of side force direction between the results computed by the formula uesd in [5] and those obtained by the present study. This graph also supports our conculusions.

5. Acknowledgment

The authors are grateful to Dr. Ryutaro Himeno of Riken for his valuable suggestions and permission for the use of the grids employed in his previous paper.

References

[1] T.Mizota et al: Journal of Wind Engineering 62(1995), 3-13
[2] T.Mizota et al: Journal of Wind Engineering 62(1995), 15-21
[3] R.Himeno et al : Proc. 12th Symposium of Computational Fluid Dynamics(1998), 311-312
[4] R.Himeno et al : Nagare 20(2001), 430-434
[5] D.Nishikiori et al : Journal of Wind Engineering 99(2004), 105-106
[6] F.H.Harlow and J.E.Welch: Phys. Fluid 8 (1965) 2182-2189
[7] T.Kawamura and K.Kuwahara AIAA paper 84-0340

Kanako Denbo
Research Institute of Systems Planning
Kasuya Bldg. 2-9, Sakuragaoka-cho, Shibuya-ku, Tokyo 150-0031 JAPAN
denbo@isp.co.jp

Tetuya Kawamura
Ochanomizu University
2-1-1 Ohtsuka, Bunkyo-ku, Tokyo 112-8610, JAPAN
kawamura@is.ocha.ac.jp

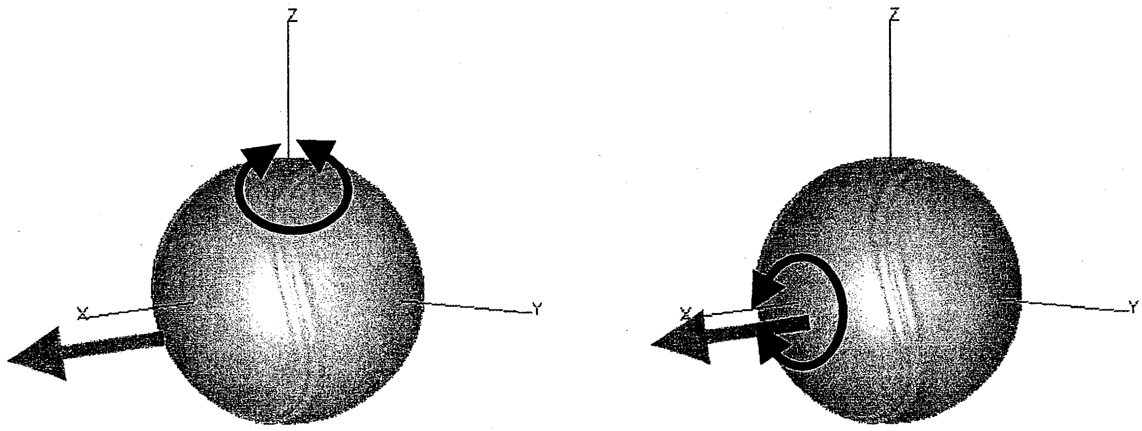

Fig. 1 Knuckleball with (a) side spin and (b) rifle spin
(a) Side Spin (b) Rifle Spin

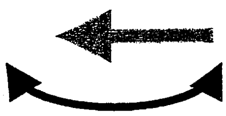

: Moving Directiom

: Direction of Rotation

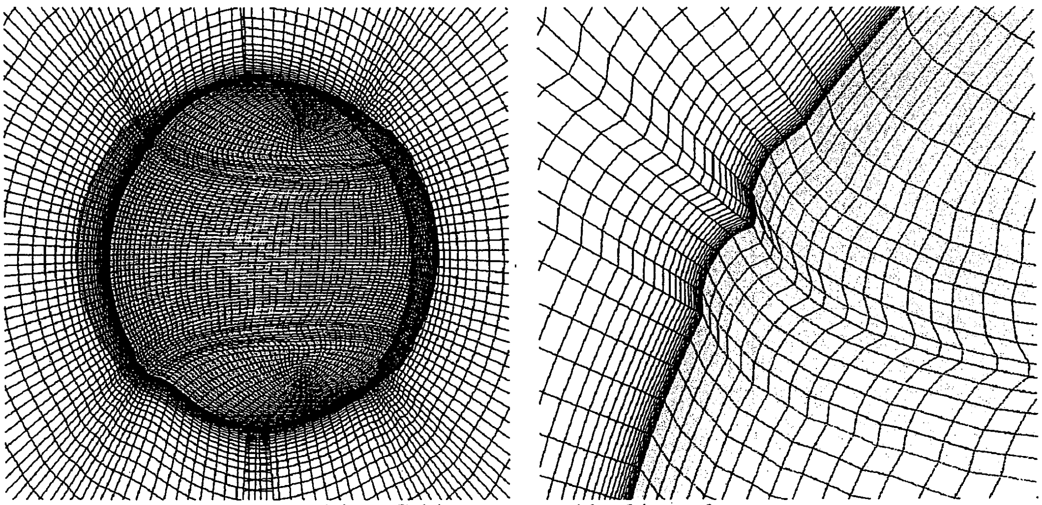

Fig.2 Grid system used in this study
(a)Grid near the ball (b) Close-up view of fig.2(a)

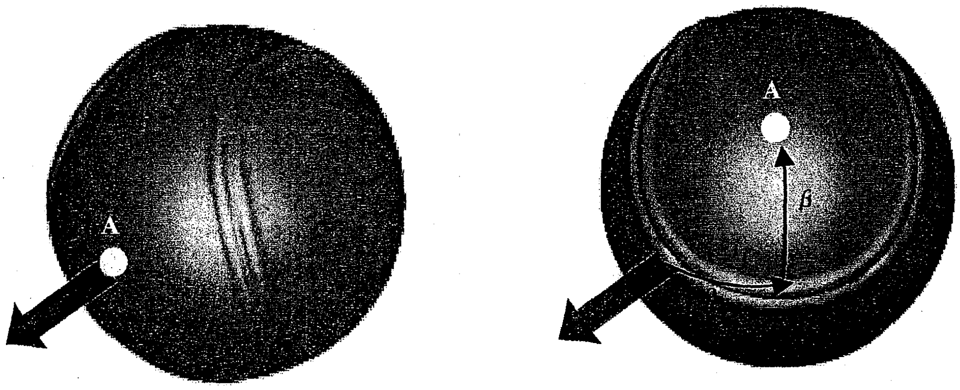

(1) $\alpha = 0°$, $\beta = 0°$ (2) α and β with non-zero values

Fig.3 : Definition of α and β

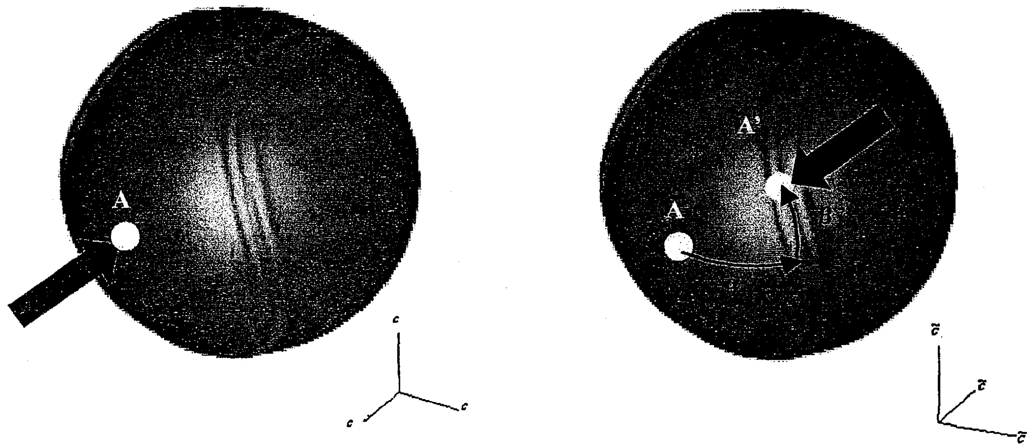

(1) $\alpha' = 0°$, $\beta' = 0°$ (2) α' and β' with non-zero values

Fig.4 : Definition of α' and β'

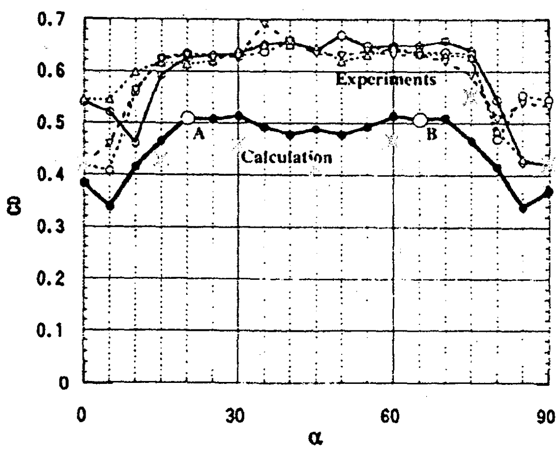

Fig.5 : Drag coefficients for various degrees of α ($\beta = 0°$)

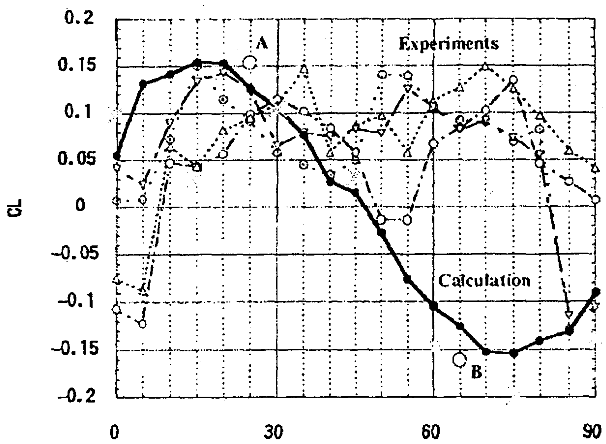

Fig.6 : Lift coefficients for various degrees of α ($\beta = 0°$)

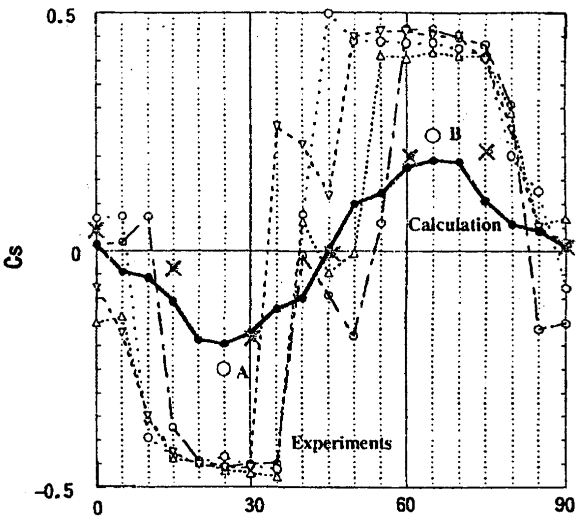

Fig.7 : Side coefficients
for various degrees of α (β =0°)

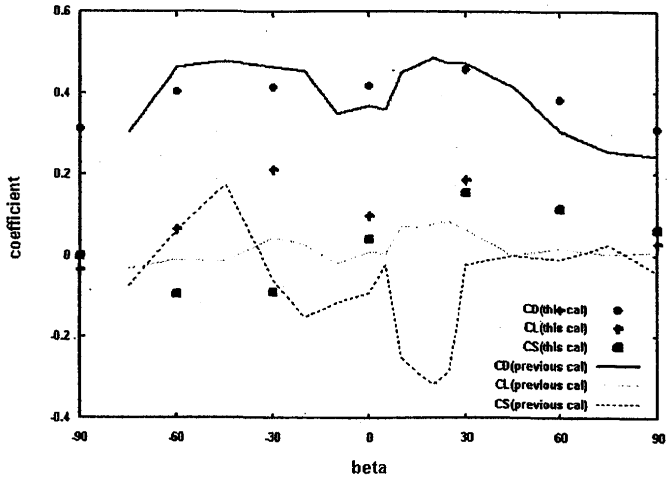

Fig.8 : Drag coefficients
for various degrees of β (α =0°)

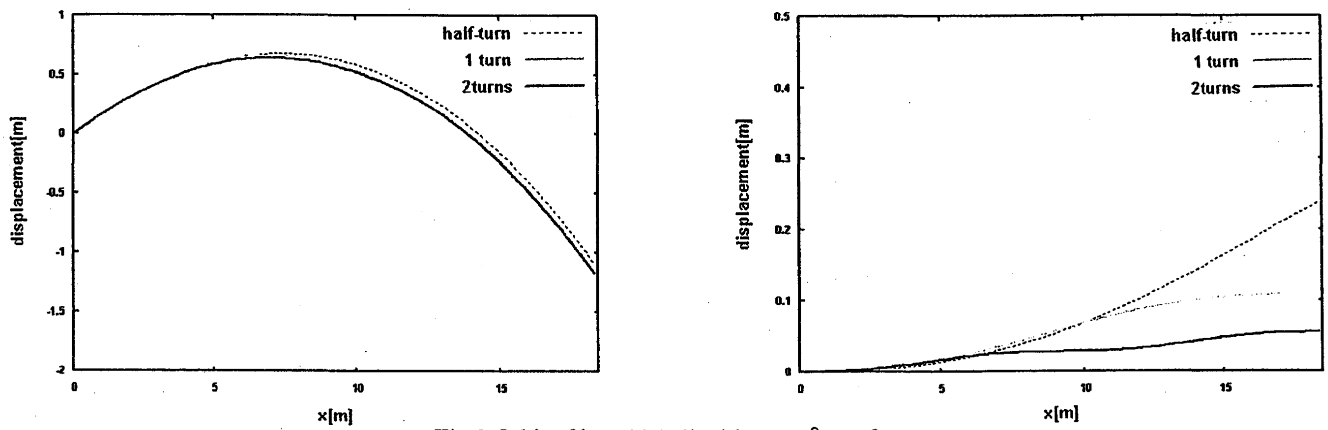

Fig.9 Orbit of knuckleball with α =0° , β =0
(a) Displacement of perpendicular direction
(b) Displacement of side force direction

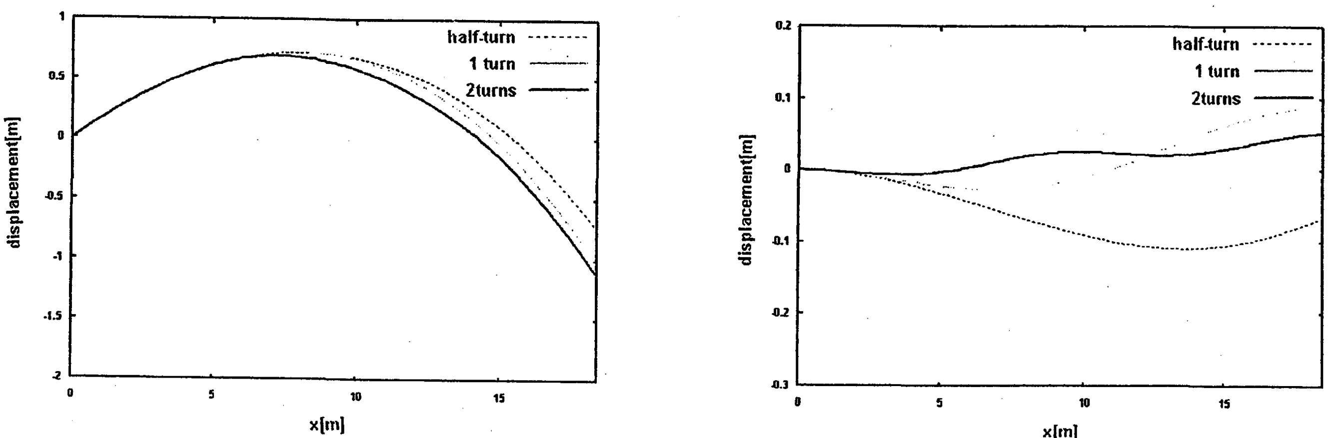

Fig.10 Orbit of knuckleball with α =30° , β =0°
(a) Displacement of perpendicular direction
(b) Displacement of side force direction

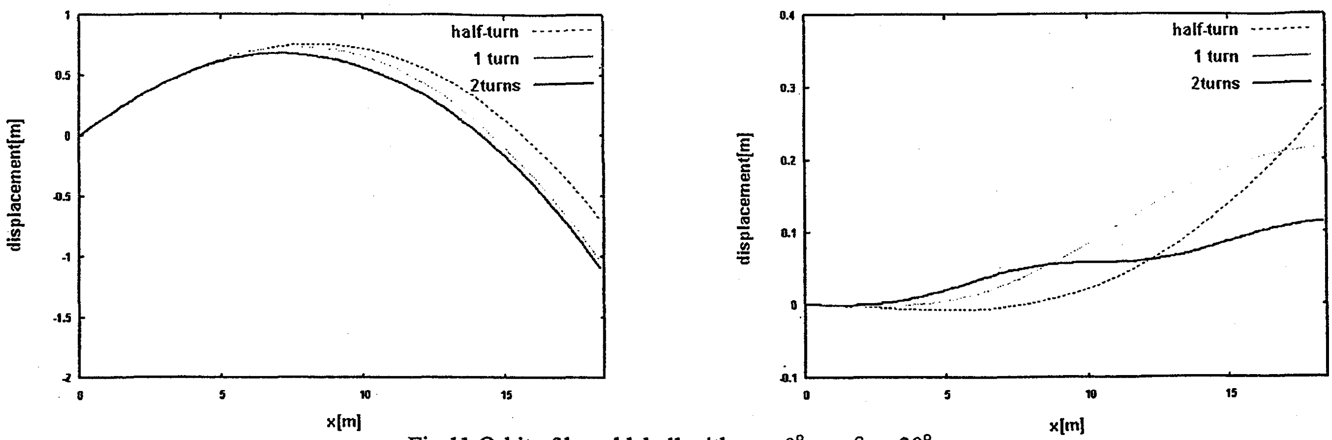

Fig.11 Orbit of knuckleball with α=0° , β = -30°

(a) Displacement of perpendicular direction (b) Displacement of side force direction

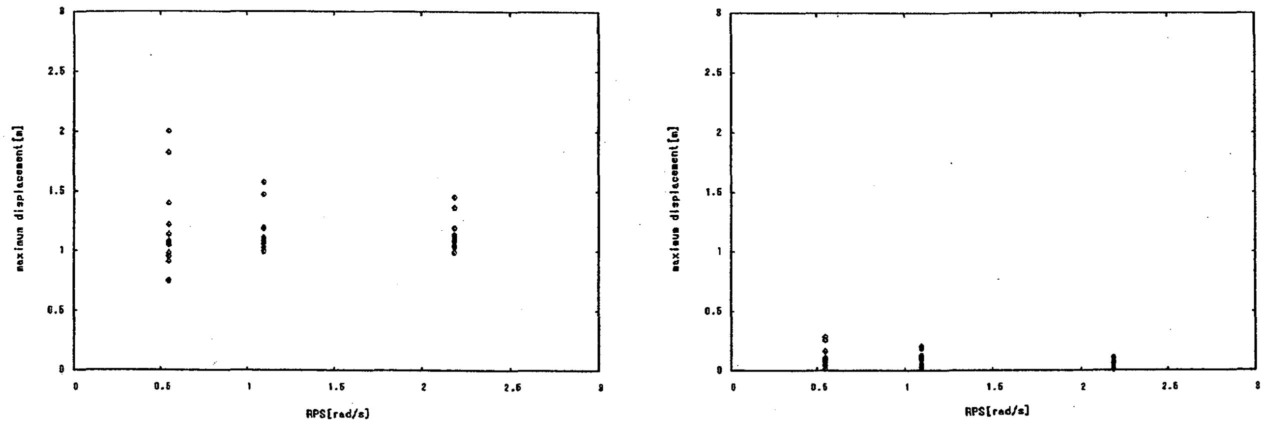

Fig.12 Maximum displacement

(a) Perpendicular direction (b) Side force direction

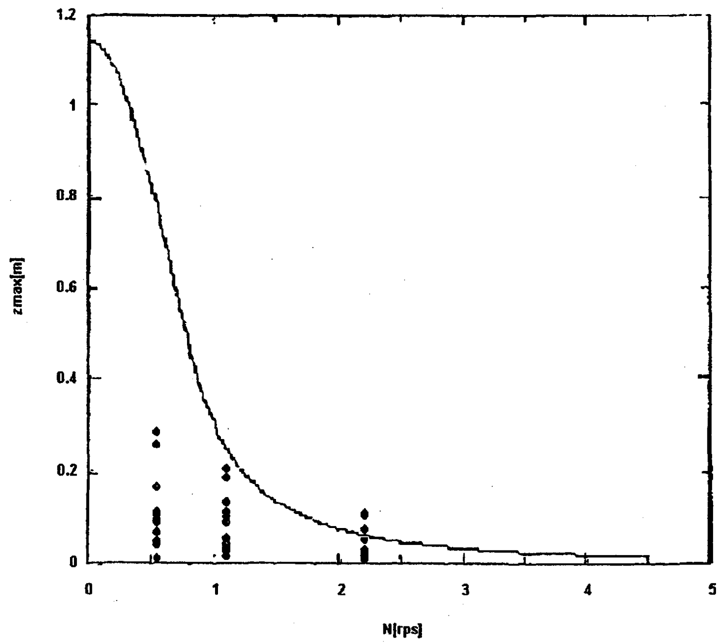

Fig.13 Comparison of side force direction